PATENT APPLICATION
Docket No.: NC 95,937

IN THE UNITED STATES PATENT AND TRADEMARK OFFICE

In the application of: Yang et al.
Serial No.: 10/725,257
Filed: 12/02/2003
For: NANOFABRICATION OF InAs/AlSb HETEROSTRUCTURES
Examiner: Thomas, Toniae M.
Art Group Unit: 2822

Honorable Commissioner of Patents
PO Box 1450
Alexandria, VA 22313-1450

DECLARATION UNDER 37 C.F.R. § 1.131 OF MING-JEY YANG AND CHIA-HUNG YANG

Sir:

We, the undersigned, hereby each declare that:

1. I am a co-inventor of the invention claimed in the above-identified patent application.

2. Attached is a copy of portions of my invention disclosure, which formed the basis of this patent application.

3. The certification shows my signature, which was in fact, to the best of my recollection, signed on 09/28/2001 as shown. The contents of the disclosure were complete at the time that I signed it.

4. The 4th page of the attachment discloses the actual use of acetic acid:H_2O_2:H_2O etchant on a heterostructure (lines 30-33).

5. All of the work described in the attachment was performed in the United States, a NAFTA country, or a WTO member country.

6. I further declare that all statements made herein of my own knowledge are true and that all statements made on information and belief are believed to be true, and further that these statements are made with the knowledge that willful false statements and the like so made are punishable by fine or imprisonment, or both, under Section 1001 of Title 18 of the United States

Code, and that such willful false statements may jeopardize the validity of the application or any patent issuing thereon.

8/29/05 _____
Date

_____
Ming-Jey Yang

8/29/05 _____
Date

_____
Chia-Hung Yang

ONRINST 5870.1C

RECORD AND DISCLOSURE OF INVENTION

FOR USE BY NAVY INTELLECTUAL PROPERTY OFFICE

DATE DISCLOSURE RECEIVED	NAVY CASE NO.

INSTRUCTIONS: A Navy employee should use this form when submitting an invention disclosure to the Department of the Navy. Fill in each blank with the requested information or enter "NONE" as appropriate. Original and two copies should be printed or typed and forwarded to the intellectual property office responsible for providing services to your activity. Where space on form is inadequate, enter "see attached page," use plain pages as needed, and identify item by number. When completely executed, this form becomes an important legal document useful in proving priority of invention. This form may also be used by a contractor or grantee for disclosing an invention to the Navy.

PART 1. RECORD OF INVENTION

1. INVENTOR(S)	ADDRESS	POSITION TITLE	EMPLOYER (Activity & Code No., or Company & address)
Ming-Jey Yang	13472 Bragman Rd Silver Spring, MD 20904	Electrical Engineer	NRL Code 6876
Chia-Hung Yang	ditto	Professor Coollaborator	University of Maryland

2. DESCRIPTIVE TITLE OF INVENTION

Novel Nanofabrication Scheme for InAs/AlSb Heterostructures

3. CONCEPTION, INITIAL RECORDS AND RESULTS OF FIRST MODEL

a. EARLIEST DATE AND PLACE INVENTION WAS CONCEIVED *(Identify persons and records to support date and place)*

March 2001, at NRL & UMd

b. DATE AND PRESENT LOCATION OF FIRST SKETCH, DRAWING OR PHOTO AND FIRST WRITTEN DESCRIPTION *(Such as notebook entries, etc.)*

April 24, 2001 First sample was grown by molecular-beam epitaxy @NRL

c. DATE AND PLACE OF COMPLETION OF FIRST MODEL, PROTOTYPE, PRELIMINARY SYNTHESIS, FORMULATION, ETC., AND ITS PRESENT LOCATION

July 2001 First magneto-transport measurement on the fabriated devices @UMd

d. DATE AND PLACE OF FIRST TEST OR OPERATION AND THE RESULTS *(Give name and address of witnesses, and present location of records)*

4. OTHER RECORDS *(Notebook entries, descriptions, reports, drawings, etc.)*

IDENTIFICATION	DATE OF DOCUMENT	PRESENT LOCATION

5. OTHER INDIVIDUALS TO WHOM INVENTION WAS DISCLOSED

NAME	ACTIVITY OR COMPANY INDIVIDUAL REPRESENTS	DATE DISCLOSED	TYPE (oral or written disclosures)
J. C. Culbertson	NRL code 6876	June 2001	oral
B. V. Shanabrook	NRL code 6870	July 16 2001	oral

NAVOCNR 5870/35 (11-88) (Rev. 5-83)

6. DATE AND PLACE OF OTHER TESTS OR OPERATIONS, AND THE RESULTS *(List name and address of witnesses and identify present location of records)*

N/A

7. IDENTIFY ANY PAST, PRESENT OR CONTEMPLATED USE, SALE, OR PUBLICATION OF THE INVENTION

~~N/A~~ Paper been submitted to Appl. Phys. Lett.

8. LIST ANY CLOSELY RELATED PATENTS, PATENT APPLICATIONS AND PUBLICATIONS OF YOURS OR OTHER PERSONS

N/A

PART II. DISCLOSURE OF INVENTION

Attach on separate sheets of paper a full and complete description of the invention, using the outline given below.

a. PURPOSE. State the purpose of the invention.

b. BACKGROUND. Describe the old methods, materials or apparatus used to perform the purpose of the invention and give their limitations and disadvantages.

c. DESCRIPTION AND OPERATION. Describe clearly and completely the best mode of the invention and give a detailed description of its operation and use. Sketches, prints, photos, or other illustrations should be attached. In the description, use reference characters to refer to components in attached illustrations.

d. ADVANTAGES AND NEW FEATURES. State the advantages of the invention over the old methods, materials or apparatus described in paragraph b above, and the features believed to be new.

e. ALTERNATIVES. Indicate any alternative methods, materials, or apparatus of the invention.

f. CONTRIBUTIONS BY INVENTORS. If this is a joint invention, indicate what contribution was made by each inventor.

PART III. CERTIFICATION OF INVENTORS

I certify that the invention disclosed herein and in the attached documents is the ☐ sole ☒ joint invention of the undersigned and that statements and answers are true to my best knowledge and belief.

Date	Signature
9-28-01	
9/28/2001	

PART IV. CERTIFICATION OF WITNESSES

I certify that the invention described herein and in the attached documents has been disclosed to and understood by me.

Date	Signature	Business Address

NAVOCNR 5870/35 (11-89) (Reverse)

Title: Novel Nanofabrication Scheme for InAs/AlSb Heterostructures

Purpose:
We report a new technique for nanofabrication in the InAs/GaSb/ALSb material system. We demonstrate with experiment and the support of a self-consistent band bending calculation that this novel scheme is highly effective for nanofabrication.

Background:
Rapidly developing nanofabrication technologies such as electron-beam and atomic-force-microscope (AFM) lithography and a variety of growth/synthesis techniques have enabled a number of material systems to exhibit mesoscopic phenomena. For example, metallic wires/rings,[1] carbon nanotubes,[2] and GaAs/AlGaAs heterostructures.[3] Among them, the GaAs/AlGaAs system is the most intensively studied due to the long mean free path (l_e) of two-dimensional (2D) electrons in heterojunctions. As a result, it is possible with current technology to fabricate ballistic one-dimensional (1D) wires, where $W<L<l_e$. Here W and L are the device's lateral confinement dimensions, width and length, respectively. The lateral confinement can be accomplished by a number of methods, e.g., mesa-etch or split-gate approaches. However, due to mid-gap pinning of the surface Fermi level (E_f^s) in the GaAs/AlGaAs system, electrons are completely depleted in heterojunctions whose metallurgical width (W_m) is narrower than 0.5 μm or so. Recently, a number of variations on nanofabrication, e.g., AFM anodization[4] and front-gate induction,[5] have been attempted to further reduce device dimensions.
The 2D electron gas in InAs quantum wells (QWs) is also known to have a long mean free path.[6] In addition, it has a number of properties that are advantageous for nanofabrication and for studying low-dimensional physics. First, the surface Fermi level pinning position in InAs, $E_f^s(InAs)$, is above the conduction band. This property makes it possible to fabricate isolated conducting wires with widths in nanometers,[7] which suggests the possibility of fabricating a complex circuit with compact dimensions. Second, a small electron effective mass ($m_e^* = 0.023\ m_0$) results in a large quantization energy, favorable for the observation of low-dimensional phenomena at higher temperatures. Finally, the relatively large Lande g-factor ($g_0 = -15$) is essential for studying spin related physics, e.g., Berry's phase resulting from the Rashba effect.[8,9]

Description And Operation:
We describea structure design and a novel process scheme that leads to a breakthrough in nanofabrication in the InAs/AlSb single QW system. Figure 1 depicts the proposed sample structure. It has a 2 μm undoped GaSb buffer, GaSb/AlSb smoothing superlattice, a 100 nm AlSb bottom barrier, a 17 nm InAs QW, a 25 nm AlSb top barrier, and three cap layers, consist of InAs/AlSb/InAs 3 nm each. Our goal is to design a structure where 2D electrons are absent in the InAs QW for as-grown samples. This is accomplished by two means: a low $E_f^s(InAs)$ and a p-doped cap layer. It has been shown that $E_f^s(InAs)$ is relatively low compared with $E_f^s(AlSb)$.[10] However, 2D electrons are still present in the well for unintentionally doped QWs that terminate with an InAs cap layer. To compensate the n-doping contribution from surface states, three cap layers are intentionally doped with Be at 10^{19} cm^{-3}. Figure 2 (a) plots the self-consistent band bending. Here we assume Be binding energies in InAs and AlSb are 20meV and 38meV,

respectively, a donor concentration of 4×10^{16} cm^{-3}, and an acceptor concentration of 5×10^{16} cm^{-3} in unintentionally doped AlSb barriers. The acceptor binding energy is assumed to be 0.4eV above the AlSb valence band maximum and $E_f^s(InAs)$ is assumed to be 0.15 eV above the conduction band minimum of the InAs cap. As shown in Fig. 2 (a), the lowest (second) subband energy, E_0 (E_1) is calculated to be 100 meV (190meV) *above* the Fermi level (E_f); i.e., the as-grown sample should be insulating.

Drastic changes in electron density in the InAs QW occur when the three cap layers are removed sequentially: Figure 2 (b)-(c) plot the self-consistent band bending for samples with different terminated layers, corresponding to the situation labeled B-C in Fig. 1. When the first 3 nm InAs cap layer is removed (called "surface-B" hereafter), the sample is terminated with a 3nm-thick AlSb layer. In this case, not only is the total Be dopant reduced, but most importantly, E_f^s is shifted upward due to a relatively high pinning position in AlSb surface. Combining these two effects brings the E_f above E_0 by 40 meV, as shown in Fig. 2(b). Here we assume $E_f^s(AlSb)$ is pinned at 0.75eV above the AlSb valence band maximum. Since the InAs conduction band minimum is 0.15eV above the AlSb valence band maximum, E_f^s is effectively changed by 0.45eV when the 3nm-thick InAs cap is removed. In other words, a change of surface material is equivalent to applying +0.45eV to a top-gate relative to the substrate. As a result, electrons are induced in the InAs QW underneath the etched region. If the subsequent 3nm-thick AlSb cap is further removed, the top-most material is InAs again (surface-C), and E_f^s is pinned back to a lower position. As plotted in Fig. 2 (c), E_f now lies just slightly below E_0. Compared to Fig. 2(a), the smaller separation between E_0 and E_f is mainly due to a reduced total Be dopant. When the last doped InAs layer is eliminated (surface-D), its band bending, plotted in Fig. 2(d), becomes similar to that of the surface-B. However, due to the absence of p-dopant and a closer distance of the InAs QW to the surface, E_f now lies further above E_0. Calculation predicts that $E_f - E_0 = 90$meV.

To test the proposed scheme, we have grown the structure on semi-insulating (001) GaAs substrates by molecular beam epitaxy with cracked As and Sb sources. The as-grown sample indeed exhibits insulating characteristic for temperature below 25K or so. We fabricated Hall bars using conventional photolithography. Two highly selective recipes, acetic acid: H_2O_2: H_2O for InAs and HF: H_2O_2: lactic acid for AlSb, are used to produce different terminated surfaces for three Hall bars, called samples B, C and D, corresponding to label of the surface in Fig. 1. Bonding pads are defined by the second photolithograph level, where all the cap layers and the top AlSb barrier are etched off, followed by metal evaporation on the InAs QW surface and lift-off. The inset of Fig. 1 displays the schematic diagram of the lateral confinement potential for sample B. The exact profile requires a 2D self-consistent calculation and an understanding of the detailed impurity concentrations in each layer.

To characterize these three Hall bars, we carried out magnetotransport measurements at 4.2 K using a conventional four-terminal lock-in technique with a current range of 10-100 nA at 17 Hz. As predicted, sample C is highly resistive, however, not insulating. The resistivity is measured to be > 200 kΩ-cm. Figure 3(a) and (b) show the longitudinal (ρ_{xx}) and transverse (ρ_{xy}) magnetoresistance for sample B and D. Both samples exhibit zero ρ_{xx} and a quantum plateau in ρ_{xy} at integer filling factors, indicating a well defined lateral confinement for edge current. The 2D electron density and mobility for sample B are found to be 4.9×10^{11} cm^{-2} and 2.0×10^5 cm^2/Vs, respectively, corresponding to l_e = 2.3

μm. By comparison, both density and mobility are roughly doubled in sample D, 1.1×10^{12} cm^{-2} and 4.3×10^{5} cm^2/Vs, leading to l_e = 7.5 μm. The obtained densities imply Fermi energies of 43 meV and 88 meV, respectively. These values are in good agreement with the band bending calculation, indicating that the parameters assumed in the calculation, such as impurity concentration and E_f^s are realistic.

With a clear understanding to our sample system, we have further fabricated a number of nanostructures by electron-beam lithography using PMMA as the etching mask. The left inset of Fig. 4 (a) shows an AFM image of a ring with a diameter (d_{ring}) of 1 μm. The boundary is smooth on the order of a few nanometers. A cross-section profile analysis indicates W_m = 137 nm and, as expected, a 3nm trench for the ring area. Figure 4 (b) shows the Aharonov-Bohm interference for a 1μm-diameter ring with W_m ~ 90 nm at 2K, where the background magnetoresistance has been subtracted. The oscillations, whose amplitude is about 1.5% of the total signal, are strongly suppressed beyond 2.5T. Figure 4 (c) is the Fourier transform spectrum of the oscillations below 0.25T, where $W_m/2$ is still larger than the magnetic length. It contains spectral density for aperiodic fluctuations, *h/e*, *h/2e* and *h/3e* oscillations. Note that the *h/e* peak, centered at 183 T^{-1}, has an extremely narrow full width of 20T^{-1}, as opposed to 76 T^{-1}, an estimate based on $\Delta B^{-1} = \pi\, d_{ring}\, W_m/(h/e)$. The observed ΔB^{-1} implies a $W \approx 30$ nm conducting channel.

Advantages And New Features:

Although nanotechnology is a rapidly developing field, effort in InAs nanofabrication has been limited. We have recently fabricated InAs conducting wires and rings as well as double-barrier-resonant tunneling dots with a minimum dimension of 30 nm using e-beam lithography and reactive-ion etching (RIE).7 However, the electron mean free path is decreased as the wire width is reduced as a result of damage on the sidewalls and on the top surface during dry etching and O_2 ashing. Ultra smallness is obtained at the expense of material quality, a drawback for practical applications. Since chemical etching is known to cause no damage, we have attempted to isolate InAs wires using 20 nm deep wet etching. Unfortunately, marginal control of sidewall roughness hinders this practice for deep submicron device fabrication. Generally speaking, the deeper the etched pattern is, the rougher the sidewall will be. As a result, chemical etching is rarely applied to nanofabrication. Moreover, lateral isolation by the physical isolation of an InAs QW may not be the ideal choice since the conducting electrons would be in close proximity to surface states and suffer from excess scattering.

With this new fabrication scheme, no additional surface states are created and the edge of the 1D electrons is defined by the electrostatic potential. Consequently, the electron mean free path is expected to be insensitive to the wire width and the material quality will not be degraded by the additional lateral confinement. The technique is simple, yet very flexible and allows creation of novel nanostructures such as dots with diameters of 16 nm would contain only one electron. This dimension, achievable by modern lithography techniques, is probably a lower bound since the lateral depletion width has not been considered. In addition, the structure discussed in this paper can be modified so that the starting density can be lower after the shallow wet etching. We believe our breakthrough will lead to a new avenue for spintronic research. In addition, the technique described here can be applied to various semiconductor heterostructures as long as a proper combination of cap layers is available.

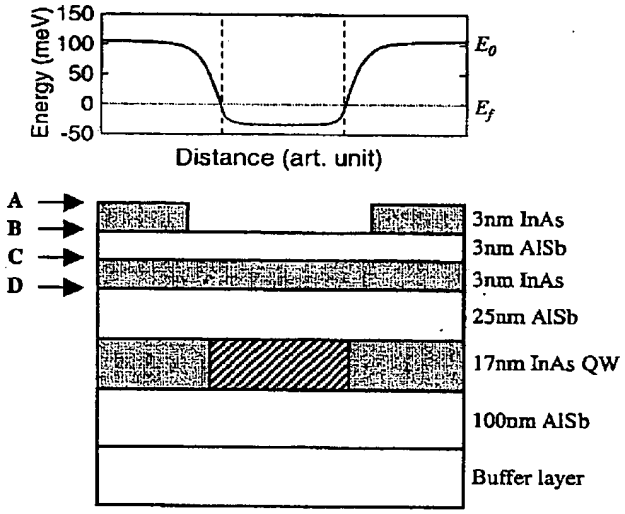

Fig. 1 Schematic diagram of the sample structure (not to scale), where A, B, C and D represent different terminated surfaces. The hatched area indicates the induced electrons by a 3nm shallow wet etch. The inset depicts the lateral confinement, where two dashed lines mark the edges of the conducting channel.

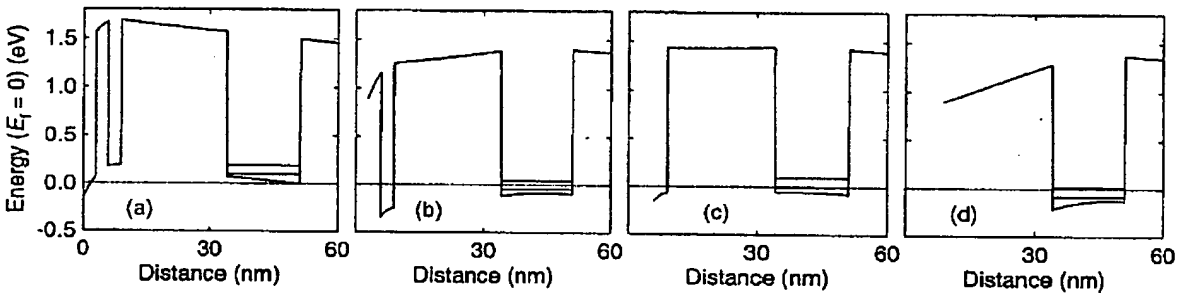

Fig. 2 The self-consistent band bending (a)-(c) for different terminated surfaces A-D, indicated in Fig. 1. Two solid lines in the InAs QW show the two lowest subbands.

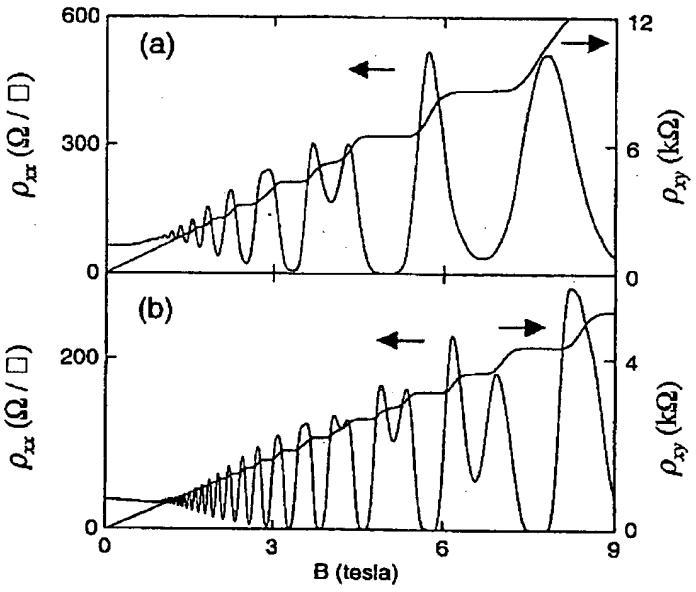

Fig. 3 (a) and (b) show the magnetoresistance data for Hall bars with terminated surfaces B and D, respectively.

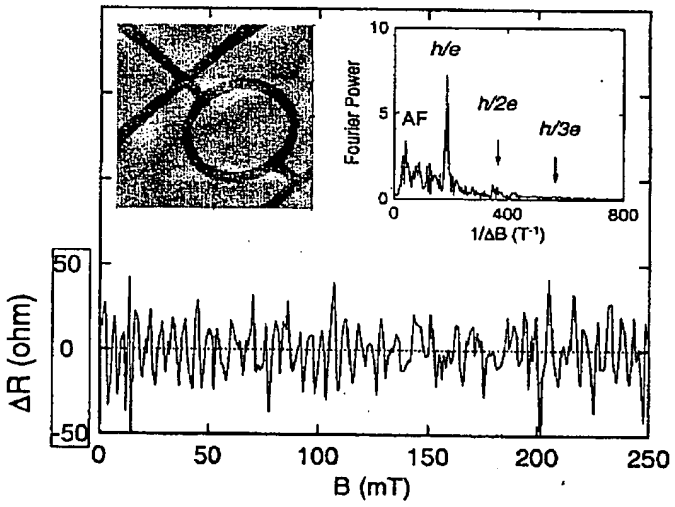

Fig. 4 The Aharonov-Bohm oscillations measured in a 1mm-diameter annulus. The left inset shows a 2mm×2mm AFM image. The right inset is the Fourier spectrum that reveals signals from aperiodic fluctuations (AF), fundamental oscillation, h/e, and higher harmonics, h/2e and h/3e.